

RESEARCH ARTICLE

# Chromosome Condensation 1-Like (*Chc1L*) Is a Novel Tumor Suppressor Involved in Development of Histiocyte-Rich Neoplasms

David R. Spillane<sup>1,2</sup>, Ding Yan Wang<sup>3</sup>, Susan Newbigging<sup>4</sup>, Youdong Wang<sup>1</sup>, Chang-Xin Shi<sup>2\*</sup>, Hae-Ra Cho<sup>5</sup>, Hiroki Shimizu<sup>5</sup>, Anthony Gramolini<sup>3</sup>, Mingyao Liu<sup>2,3,5</sup>, Xiao-Yan Wen<sup>1,2,3\*</sup>

**1** Keenan Research Centre for Biomedical Science, Li Ka Shing Knowledge Institute, St. Michael's Hospital, Toronto, Ontario, Canada, **2** Department of Medicine & Institute of Medical Science, University of Toronto, Toronto, Ontario, Canada, **3** Department of Physiology, University of Toronto, Toronto, Ontario, Canada, **4** Centre for Modeling Human Disease, Samuel Lunenfeld Research Institute, Mount Sinai Hospital, The Toronto Centre for Phenogenomics, University of Toronto, Toronto, Ontario, Canada, **5** Latner Thoracic Surgery Research Laboratories, Toronto General Research Institute, University Health Network, Toronto, Ontario, Canada

☞ These authors contributed equally to this work.

✉ Current address: Department of Hematology/Oncology, Mayo Clinic, Scottsdale, Arizona, United States of America

\* [x.wen@utoronto.ca](mailto:x.wen@utoronto.ca)



**OPEN ACCESS**

**Citation:** Spillane DR, Wang DY, Newbigging S, Wang Y, Shi C-X, Cho H-R, et al. (2015) Chromosome Condensation 1-Like (*Chc1L*) Is a Novel Tumor Suppressor Involved in Development of Histiocyte-Rich Neoplasms. PLoS ONE 10(8): e0135755. doi:10.1371/journal.pone.0135755

**Editor:** Javier S Castresana, University of Navarra, SPAIN

**Received:** May 20, 2015

**Accepted:** July 25, 2015

**Published:** August 20, 2015

**Copyright:** © 2015 Spillane et al. This is an open access article distributed under the terms of the [Creative Commons Attribution License](https://creativecommons.org/licenses/by/4.0/), which permits unrestricted use, distribution, and reproduction in any medium, provided the original author and source are credited.

**Data Availability Statement:** All relevant data are within the paper and its Supporting Information files.

**Funding:** This work is funded by a grant from the Multiple Myeloma Research Foundation (MMRF) to XYW (<http://www.themmf.org/>).

**Competing Interests:** The authors have declared that no competing interests exist.

## Abstract

Human chromosomal region 13q14 is a deletion hotspot in prostate cancer, multiple myeloma, and chronic lymphocytic leukemia. This region is believed to host multiple tumor suppressors. Chromosome Condensation 1-like (*CHC1L*) is located at 13q14, and found within the smallest common region of loss of heterozygosity in prostate cancer. Decreased expression of *CHC1L* is linked to pathogenesis and progression of both prostate cancer and multiple myeloma. However, there is no direct evidence for *CHC1L*'s putative tumor suppressing role in current literature. Presently, we describe the generation and characterization of *Chc1L* knockout mice. *Chc1L*<sup>-/-</sup> mice do not develop cancer at a young age, but bone marrow and spleen cells from 8–12 week-old mice display an exaggerated proliferative response. By approximately two years of age, knockout and heterozygote mice have a markedly increased incidence of tumorigenesis compared to wild-type controls, with tumors occurring mainly in the spleen, mesenteric lymph nodes, liver and intestinal tract. Histopathological analysis found that most heterozygote and knockout mice succumb to either Histiocytic Sarcoma or Histiocyte-Associated Lymphoma. Our study suggests that *Chc1L* is involved in suppression of these two histiocyte-rich neoplasms in mice and supports clinical data suggesting that *CHC1L* loss of function is an important step in the pathogenesis of cancers containing 13q14 deletion.

## Introduction

Chromosome condensation 1-like (*CHC1L*, aka *RCBTB2*) is an uncharacterized gene residing at 13q14.3 in humans. This region is frequently lost in several human cancers, including B cell chronic lymphocytic leukemia (CLL) (70% incidence of deletion [1]), multiple myeloma (MM) (40–50% incidence [2]), and prostate cancer (PC) (33% incidence [3]), as well as myeloid disorders and dendritic sarcomas [4, 5]. The high frequency of deletion suggests the existence of tumor suppressor genes residing in this region.

In an effort to identify candidate tumor suppressors, several groups have mapped 13q14 deletions [6, 7]. *CHC1L* is located within the smallest common region of loss of heterozygosity (LOH) in PC [8]. Expression is decreased at least 2-fold in 58% of all PC tumors, as well as in the three prostate cancer cell lines LNCaP, DU145, and PC3 [8]. Among PC tumors with LOH at 13q14, *CHC1L* is significantly down-regulated in 78% of cases [8]. Additionally, low expression levels of *CHC1L* are frequently observed in MM patients [9].

The murine orthologue encodes a protein of 551 amino acids, sharing 95% identity with human *CHC1L*. Mouse studies have proposed a role during acrosome formation in developing spermatocytes through regulation of nuclear transport [10]. *CHC1L* possesses RCC1-like repeats on its N-terminal and BTB domains on its C-terminal [11].

While previous studies have shown an association between cancer occurrence and *CHC1L* deletion/under-expression, a reverse genetic approach is needed to show the contribution of loss of function to tumorigenesis in order to validate its hypothesized tumor suppressive function. Here, we describe the generation and characterization of *Chc1L* knockout mice.

## Materials and Methods

### Experimental animals

Experimental mice were generated on a C57/BL6 background. The protocol was approved by the Ethics Board of the Animal Resource Center at Princess Margaret Hospital (Toronto, ON) (Protocol ACC418), where the animals were housed. The Animal Resource Center is fully accredited by the Canadian Council for Animal Care. Animals were maintained on standard feed and water *ad libitum*, in a clean, temperature-controlled environment with standard day-light cycles.

To minimize stress, animals were euthanized in their home cages using carbon dioxide, followed by cervical dislocation as secondary euthanasia. All efforts were made to minimize suffering. Dissections were performed by an experience technician and graduate students in a biosafety cabinet.

### Gene targeting strategy

Murine *Chc1L* contains a start codon in exon 4, and a second ATG in exon 5. In order to prevent the second ATG from assuming start codon activity, both exons were flanked by unidirectional loxP sites (Fig 1A). ES cells were electroporated with the targeting vector and selected by neomycin resistance. Successful knockin was confirmed by Southern Blot (Fig 1B).

Gene targeted ES cells were injected into embryos which were implanted into pseudopregnant mice. Gene targeting in the progeny was confirmed by Southern Blot (Fig 1C). *Chc1L*<sup>loxP/+</sup> mice were then crossed to a line expressing Cre recombinase under the *Blimp1* promoter, active in germ cells [12, 13]. The F2 generations possessed nonconditional deletion of exons 4 and 5.

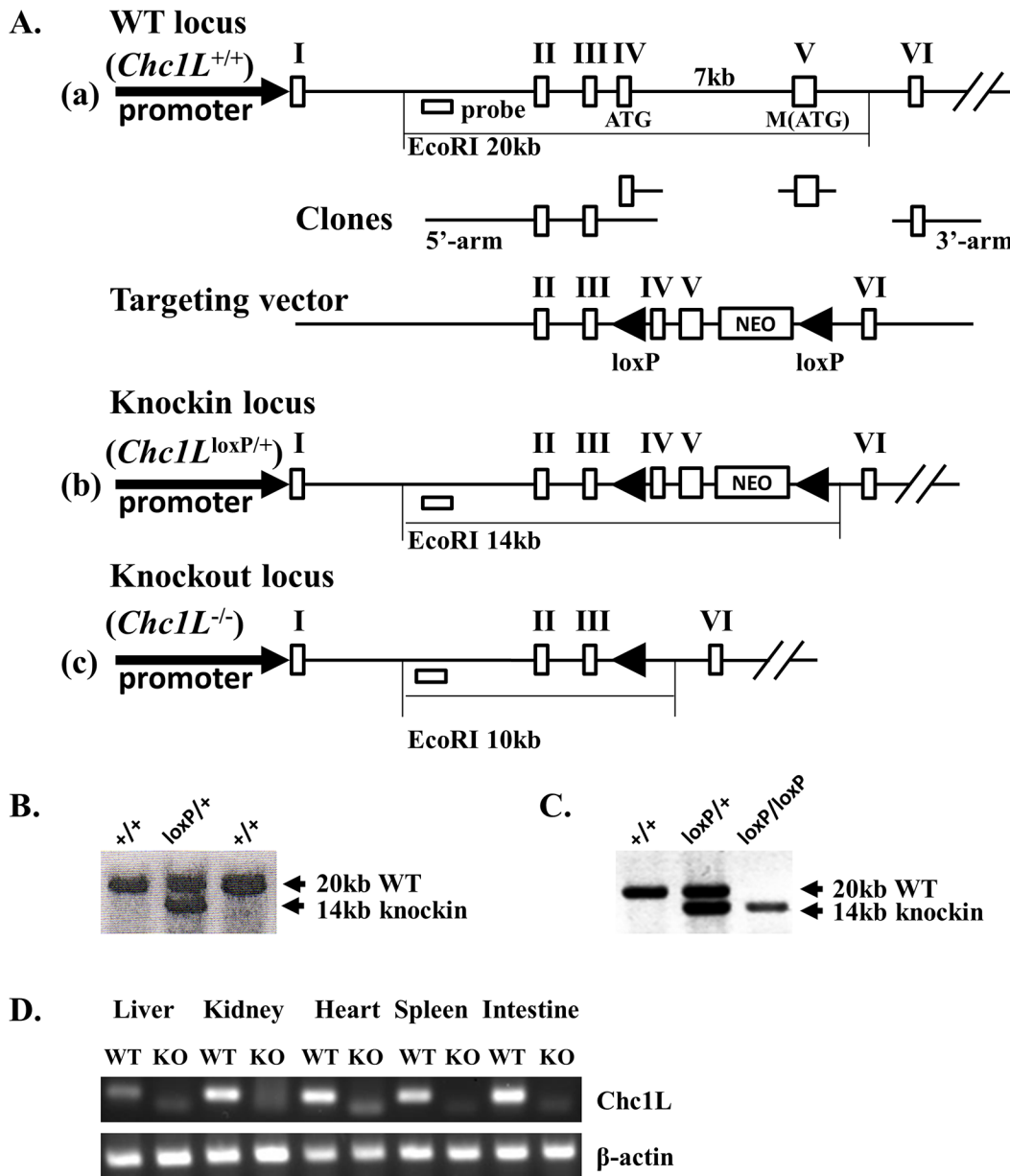


**Fig 1. Generation of *Chc1L*<sup>-/-</sup> knockout mice by gene targeting.** A) Gene targeting strategy. (a) The start codon is located in exon 4 of murine *Chc1L*, and a second ATG codon is in exon 5. EcoRI digestion produces a gene fragment of 20 kb. Deleting 6kb of intron 4, a gene targeting vector was constructed, with unidirectional loxP sites flanking exons 4 and 5. (b) The gene-targeted locus produces a 14 kb fragment upon digestion with EcoRI. (c) Exon 4, intron 4 and exon 5 are lost following Cre-mediated recombination. B) Confirmation of gene targeting in ES cells. Successful knockin of neomycin-selected ES cells was detected by Southern Blot using a 5' probe, visualizing a 20kb WT locus fragment, and a 14kb gene-targeted fragment. C) Confirmation of gene targeting in mice. Gene knockin was confirmed in mice again using Southern Blot. D) Confirmation of loss of *Chc1L* expression. Loss of *Chc1L* expression was confirmed by RT-PCR.

doi:10.1371/journal.pone.0135755.g001

### Genotyping strategy

Tissue was incubated overnight in lysis buffer at 55°C (1.5 mM MgCl<sub>2</sub>, 50 mM KCl, 10 mM Tris-HCl pH 8.3, 20 μg/mL protease K). Intron 4 primers detected the wild-type allele (Int4F 5' - GTGTTACTTTTGCCCGTGGT-3', and Int4R 5' - GTGACAGGGCAAACCAAGTT-3'). Introns 3 and 5 are brought into close enough proximity to be amplified in the knockout but

not wild-type tissues (DelF 5' - TTCGCTACCTTAGGACCGTTA-3' , DelR 5' - GGGTACC GAATTCCTCGAC 3' ).

## RT-PCR

Verification of knockout at the protein level was difficult due to a lack of specificity among commercially available antibodies. Therefore, RT-PCR was used. Tissues were collected in RNase-free conditions and snap frozen. RNA was collected using QIAGEN RNeasy Plus kit (Qiagen, Cat. No. 74134; Venlo, Limburg, Netherlands) according to manufacturer's protocol. RNA integrity was verified on an Agilent 2100 Bioanalyzer (Santa Clara, CA, USA). RNA was reverse transcribed using Applied Biosystems' High Capacity cDNA Reverse Transcription Kit (Applied Biosystems, 4368814; Carlsbad, CA, USA). Two sets of primers were used for detection of the wild-type transcript by amplifying around the exon 4/5 splice site (F1 5' -AGGGA CTGCACAGGACTGAT-3' , R1 5' - CAAGCCTGACGAATCAACTG-3' and F2 5' - TGGAA GAAGAAGTGCCCTGGT-3' , R2 5' -GGCCACTTCCACATCTAA-3' ). The identity of the amplicon was confirmed by sequencing.

## MTT assay

Cells were isolated from age- and sex-matched mice between 8–12 weeks of age. Bone marrow and spleen cells were cultured in triplicate at  $2 \times 10^5$  cells per well in a 96-well plate with 200  $\mu$ L DMEM/10%FBS/1%Antibiotic + LPS for 48 hours. 10  $\mu$ L MTT solution (5 mg/mL MTT (Invitrogen, catalogue number M-6494; Carlsbad, CA, USA) in PBS) was added to each well, and cultured for 4 hours. 100  $\mu$ L solubilisation solution (10% SDS in ddH<sub>2</sub>O+100  $\mu$ L of 37% HCl per 100 mL) was added to each well, and cultured for 4 hours. OD was read at 570 nm. Experiment was performed on three pairs of animals.

## Histology

All tissues were collected into formalin and fixed overnight. Tissues were embedded in paraffin, sectioned, and stained by hematoxylin and eosin. For immunohistochemistry (IHC), standard tissue sections were deparaffinized, rehydrated and post-fixed in 10% neutral-buffered formalin for 1 hour. Sections were soaked in 10mM citrate buffer (pH 6.0) at 85°C for 3 hours (for Mac-2 only). Slides were air-dried and washed in PBST, then soaked in 3% hydrogen peroxide in methanol for 30 minutes. Slides were blocked using Dako protein block (Dako: catalogue number X0909; Santa Clara, CA, USA). 1:100 diluted monoclonal rat anti-Mac-2 (Cedarlane: catalogue number CL8942AP; Burlington, ON, CA), rat monoclonal anti-F4/80 (ABCAM: catalogue number AB6640; Cambridge, England, UK) or rat monoclonal anti-B220 (BD Bioscience: catalogue number 550286; Franklin Lakes, NJ, USA) was pipetted onto slide surface and incubated overnight at 4°C. The slides were washed and incubated in 1:100 anti-rat IgG-biotin (Vector Labs: catalog number BA-4001; Burlingame, CA, USA) at room temperature for 60 minutes. A and B from kit ABC (Vector Labs: catalogue number PK-6100; Burlingame, CA, USA) were pipetted onto slides, and incubated 30 minutes room temperature. Slides were immersed in DAB colour development solution, then washed in distilled water. Slides were counterstained with hematoxylin, dipped in 1% acid alcohol, and then immersed in Scott's tap water. Finally, slides were dehydrated and cleared, then coverslipped with Permount.

## Statistical methods

P values for tumor incidence were calculated using the Chi-squared test with a 3x2 contingency table.



P values for MTT cell survival were calculated using the two-tailed student's T test.

## Results

### Chc1L-deficiency increases incidence of tumorigenesis

To examine the role of *Chc1L* in tumorigenesis, we knocked out the murine *Chc1L* gene by germ-line deletion of the ATG-containing exons 4 and 5 through Cre-mediated recombination (Fig 1A). Successful gene targeting in ES cells and knockout mice was confirmed by Southern Blotting (Fig 1B and 1C), and loss of expression was validated by RT-PCR and sequencing (Fig 1D). *Chc1L*<sup>+/+</sup>, *Chc1L*<sup>+/-</sup> and *Chc1L*<sup>-/-</sup> mice were born at Mendelian frequency, indicating that they have viable embryonic development.

Histopathological analysis of spleen, lymph node and liver tissue was performed with tissues isolated from *Chc1L*<sup>-/-</sup> mice aged 8–12 weeks. No visible general pathology was observed, and there was no evidence of early neoplastic events.

However, as our initial interests were MM and CLL, when spleen and bone marrow cell suspensions from 8–12 week old mice were cultured in the presence of lipopolysaccharide (LPS), *Chc1L*<sup>-/-</sup> cells had a consistently increased survival rate compared to controls (Fig 2A).

Allowing for neoplastic progression, mice were sacrificed at 18–26 months, and detailed necropsies were performed. Tumors were significantly more prevalent in *Chc1L*<sup>+/-</sup> (10/18) and *Chc1L*<sup>-/-</sup> (20/25) mice, compared to *Chc1L*<sup>+/+</sup> controls (5/19),  $p < 0.01$  (Fig 2B). Tumors were most commonly observed in the spleen (*Chc1L*<sup>+/-</sup>: 8/18; *Chc1L*<sup>-/-</sup>: 7/25), mesenteric lymph nodes (*Chc1L*<sup>+/-</sup>: 6/18; *Chc1L*<sup>-/-</sup>: 9/25), liver (*Chc1L*<sup>+/-</sup>: 3/18; *Chc1L*<sup>-/-</sup>: 5/25), and intestines (*Chc1L*<sup>+/-</sup>: 6/18; *Chc1L*<sup>-/-</sup>: 2/25) (Fig 2C). Although overall tumor incidence in *Chc1L*<sup>+/-</sup> mice was lower than in *Chc1L*<sup>-/-</sup> mice, individual *Chc1L*<sup>+/-</sup> mice had a greater number of organs with tumors (Fig 2D). There was no indication of PC development.

### Chc1L disruption leads to histiocyte-rich neoplasms

Conventional histopathological studies were performed on H+E-stained tumor sections. Representative tumors from affected tissues (spleen, lymph node, liver) were collected from *Chc1L*<sup>+/-</sup> (n = 8) and *Chc1L*<sup>-/-</sup> (n = 11) mice and compared to the same tissues of age- and sex-matched *Chc1L*<sup>+/+</sup> mice (n = 4). Spleen and mesenteric lymph nodes were frequently enlarged due to proliferation of transformed cells, expanding the tissues and destroying normal architecture (Fig 3A, panels 1 and 2) (see S1 Fig for H+E controls). The liver was often involved, and many had proliferations of neoplastic cells surrounding hepatic blood vessels (Fig 3A, panel 3). Tumors found on the lower gastrointestinal tract often caused destruction of the mucosal surface (Fig 3A, panel 4).

The morphology of the tumor cells in question varies from round to spindle-shaped, with abundant eosinophilic cytoplasm and pleiomorphic (round, oval and folded) nuclei (Fig 3A, panel 5). These features are consistent with the morphology of malignant histiocytes [14].

Often, large numbers of lymphocytes were found in the histiocyte-rich neoplasms. Mott cells, plasma cells defective in immunoglobulin secretion, that are sometimes found in MM [15], were found associated with the lymphocytes in one *Chc1L*<sup>+/-</sup> mouse. Additionally, two other *Chc1L*-deficient mice had tumor cells with a plasma cell appearance, which may indicate that myeloma-like features are a component of the disease spectrum in *Chc1L*-disrupted mice. One *Chc1L*<sup>-/-</sup> mouse examined had large numbers of multinucleated giant cells admixed with the tumor cells (Fig 3A, panel 6). Extramedullary hematopoiesis was observed in the livers and/or spleens of three mice. Abundant mitotic figures and apoptotic bodies were common.

Collectively, these findings are indicative of HS. Some tumors contain both histiocytes and large numbers of lymphocytes, and were differentially diagnosed as Histiocyte-Associated

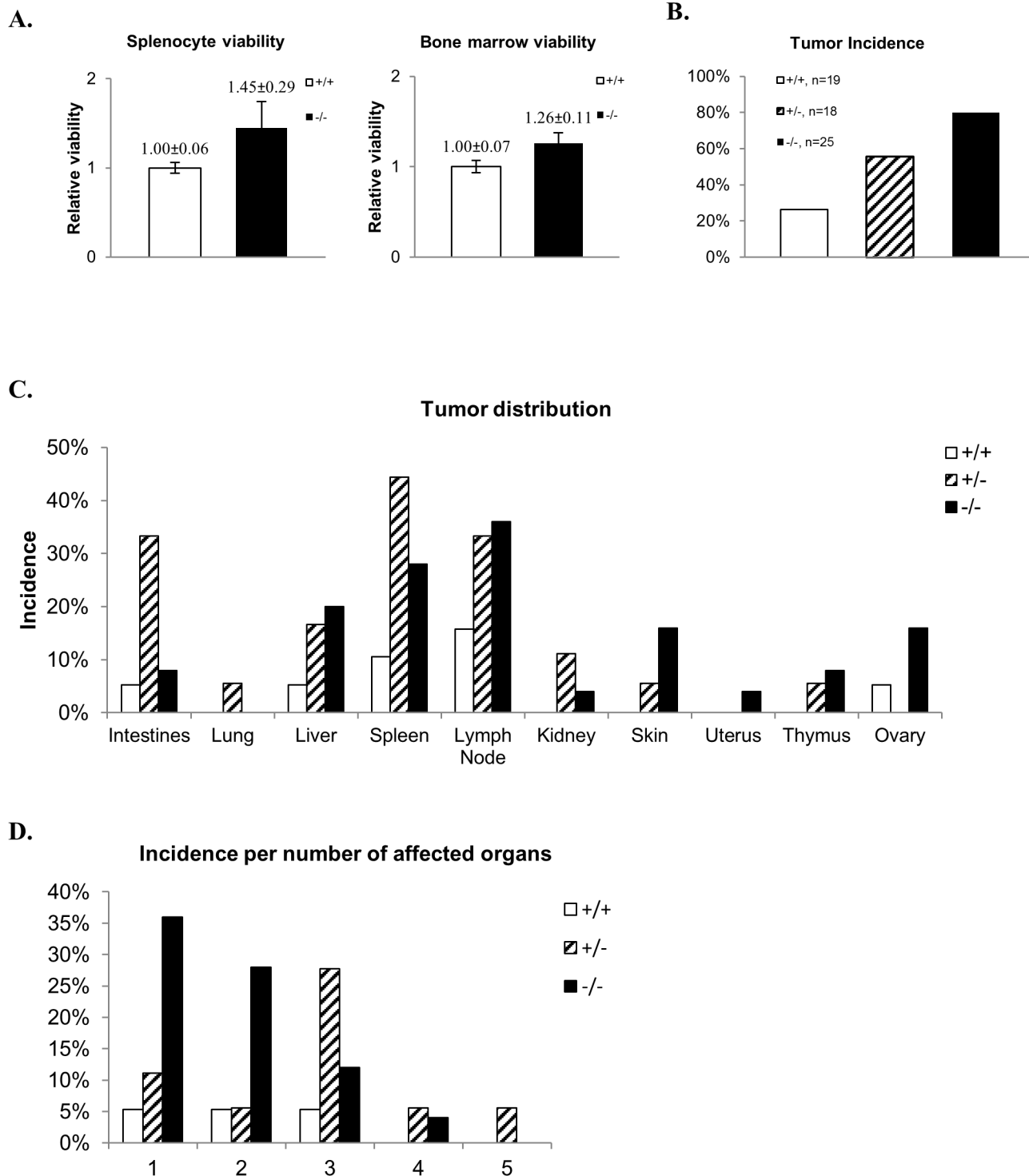
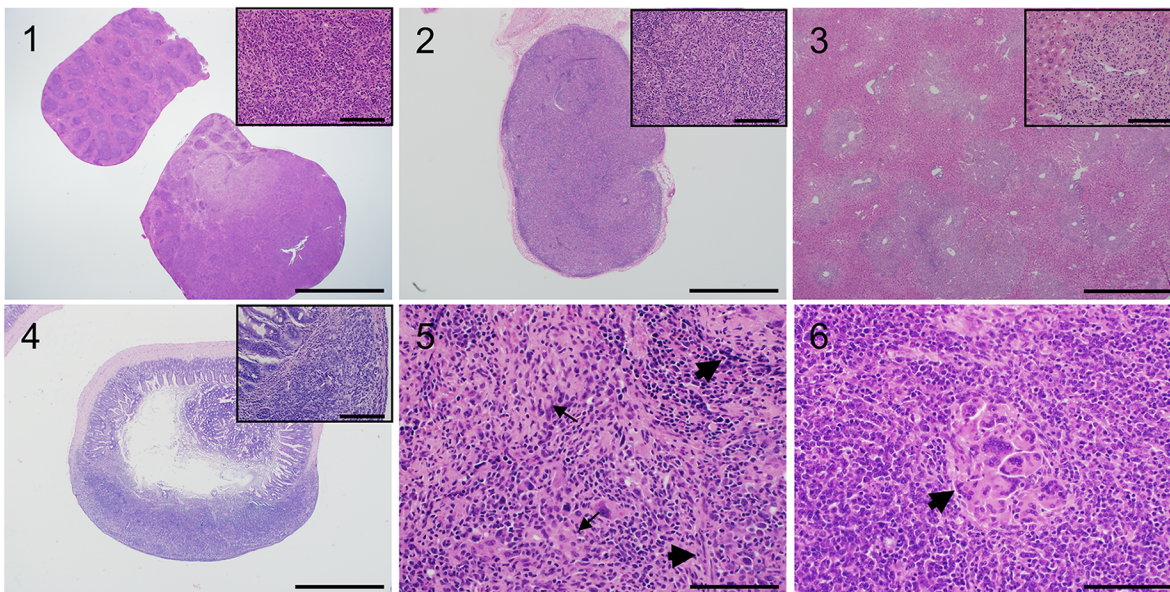


**Fig 2. *Chc1L*<sup>+/-</sup> and *Chc1L*<sup>-/-</sup> mice have elevated tumor incidence.** A) Splenocyte and bone marrow cell viability. *Chc1L*<sup>-/-</sup> splenocytes and bone marrow cells have increased viability following LPS-stimulation, compared wild-type controls (splenocyte fold-survival *Chc1L*<sup>-/-</sup>/*Chc1L*<sup>+/+</sup> = 1.45 ± 0.29, p < 0.05, n = 3; bone marrow fold-survival *Chc1L*<sup>-/-</sup>/*Chc1L*<sup>+/+</sup> = 1.26 ± 0.11, p < 0.01, n = 3). B) Tumor incidence. Tumor incidence by genotype. Incidence of observable tumors was highest in *Chc1L*<sup>+/-</sup> and *Chc1L*<sup>-/-</sup> mice (*Chc1L*<sup>+/+</sup>: 26%, *Chc1L*<sup>+/-</sup>: 56%, *Chc1L*<sup>-/-</sup>: 80%). C) Tumor distribution. Tumors were found most often in the spleen, mesenteric lymph nodes and liver. D) Incidence of multiple organs being affected. *Chc1L*<sup>+/-</sup> mice typically had multiple tumor-bearing organs.

doi:10.1371/journal.pone.0135755.g002



A.



B.

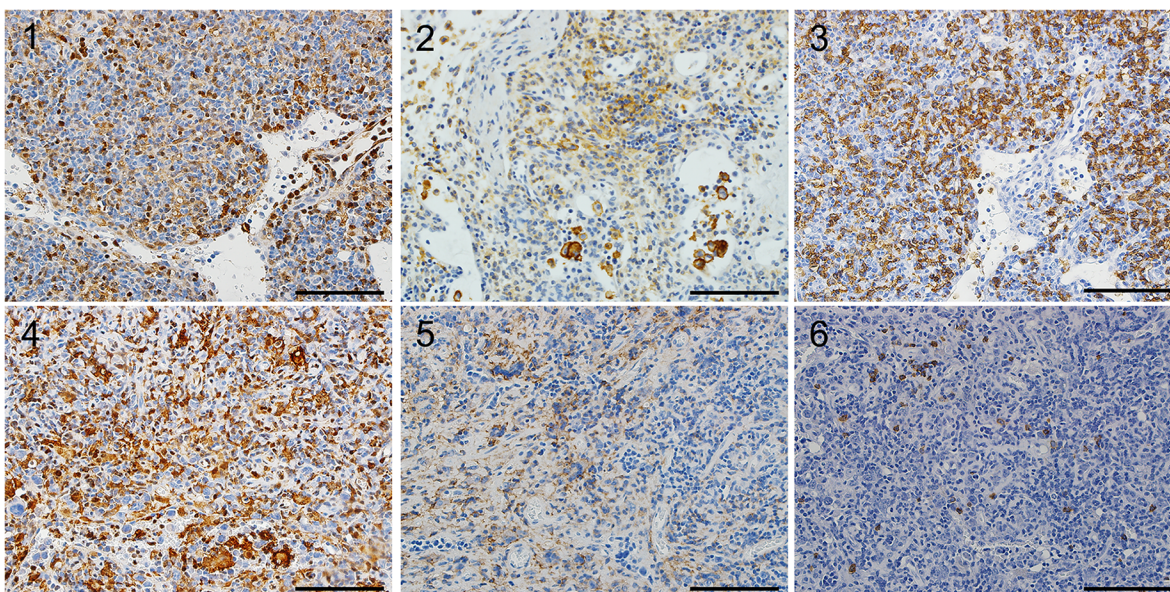


**Fig 3. *Chc1L*<sup>+/+</sup> and *Chc1L*<sup>-/-</sup> mice develop HS and HAL.** A) Representative H+E staining. Panel 1) *Chc1L*<sup>+/+</sup> and *Chc1L*<sup>-/-</sup> spleens were often enlarged, with normal structure obliterated by proliferation of tumor cells with abundant, eosinophilic cytoplasm, and irregular nuclei with open chromatin and prominent nucleoli (scale bars are 4 mm and 50  $\mu$ m). Panel 2) *Chc1L*<sup>+/+</sup> and *Chc1L*<sup>-/-</sup> lymph nodes were also enlarged, with normal structure displaced by tumor cells with morphology as described in the spleen (scale bars are 1 mm and 50  $\mu$ m). Panel 3) Frequently, multifocal areas of tumor cell infiltration that destroy the hepatic parenchyma were observed in *Chc1L*<sup>+/+</sup> and *Chc1L*<sup>-/-</sup> mice (scale bars are 1 mm and 50  $\mu$ m). Panel 4) Peyer's patch is severely enlarged by tumor cells which have destroyed the submucosa (scale bars are 1 mm and 50  $\mu$ m). Panel 5) HS cells have pleiomorphic morphology, varying from spindle shaped (wide arrows) to round (thin arrows) (scale bar is 100  $\mu$ m). Panel 6) Multinucleated giant cells (arrow) have collected in this proliferation of HS cells. Mitotic figures are abundant (scale bar is 100  $\mu$ m). See [S1 Fig](#) for H+E controls. B) Immunohistochemical staining confirms diagnosis. Panels 1–3) A lymph node differentially diagnosed with HS co-occurring with B cell lymphoma or HAL. The abnormally structured lymph node is shown, with accumulation of Mac2+ (panel 1), F4/80+ (panel 2) histiocytes admixed with B220+ (panel 3) B lymphocytes (scale bars are 50  $\mu$ m). Panels 4–6) A lymph node diagnosed with HS is shown. The enlarged lymph node has abundant Mac2+ (panel 4) and F4/80+ (panel 5) histiocytes, and only the occasional B220+ (panel 6) B cell (scale bars are 50  $\mu$ m).

doi:10.1371/journal.pone.0135755.g003

Lymphoma (HAL) or B cell lymphoma (BCL) co-occurring with HS. [Table 1](#) summarizes the histological findings in tissues collected for analysis.

Immunohistochemistry (IHC) for histiocyte markers Mac2 and F4/80 and B cell marker B220 was performed on representative tumors to confirm these diagnoses. As shown in [Fig 3B](#), a lymph node with HAL/HS+BCL contained cells stained positively for Mac2, F4/80 admixed with cells stained positively for B220. A separate lymph node with HS possessed Mac2 and F4/80 positive cells, which had displaced the native B220 positive lymphocytes of the tissue.

## Discussion

*CHC1L* is a candidate tumor suppressor gene located at human chromosome 13q14, a region frequently deleted in PC, MM and CLL. It is frequently underexpressed in MM and PC. However, there have been no studies confirming its tumor suppressive effect. In the present study, we provide the first direct evidence of its role in tumor suppression.

Employing Cre-Lox recombination, we generated a novel, non-conditional knockout mouse model for *Chc1L*. *Chc1L*<sup>-/-</sup> mice are born at expected Mendelian frequencies, and develop normally. At 8–12 weeks of age, cultured bone marrow and spleen isolates from *Chc1L*<sup>-/-</sup> mice have increased survival in response to LPS, compared to *Chc1L*<sup>+/+</sup> controls. We believe that this represents a heightened ability to proliferate, which, when compounded by additional mutations as the mice age, promotes tumorigenesis.

Indeed, at two years of age, both *Chc1L*<sup>+/-</sup> and *Chc1L*<sup>-/-</sup> mice were found to have a significantly higher incidence of grossly observable tumors compared to wild-type. Histopathological and immunohistochemical analyses determined that these mice were developing HS and HAL, or a composite of HS and BCL. There are presently no methods to distinguish HAL from a composite of HS and BCL [14]. Other murine models of HS have been found to possess an elevated incidence of BCL as a component of the tumor spectrum [16–18], suggesting that our mice with HAL/HS+BCL may actually have the latter diagnosis of simultaneous HS and BCL.

Histiocytic Sarcoma is a rare hematopoietic neoplasm, representing <1% of all human non-Hodgkin’s lymphomas [19]. Pathogenesis of human and murine HS is not well understood. In humans, there is evidence of HS developing from a B cell precursor, which trans- or de-differentiates into a malignant histiocyte. HS cells from patients with previous or co-occurring diagnosis of BCL have been found to contain lymphoma-specific genetic traits, including *t*(14:18), the genetic hallmark of Follicular Lymphoma (FL), and immunoglobulin rearrangements with common breakpoints between paired HS and FL tumors [20]. Several HS cases involving normal B cell genotypes have been detected [21–23]. Similarly, B cell immunophenotypes have been detected on human HS cells [24], including those diagnosed in the absence of BCL [25].

**Table 1. Summary of histopathological diagnoses.** *Chc1L*<sup>+/-</sup> and *Chc1L*<sup>-/-</sup> mice developed HS and HAL or HS co-occurring with BCL. *Chc1L*<sup>-/-</sup> mice developed more cases of HS, while *Chc1L*<sup>+/-</sup> mice had more diagnoses of HAL/HS+BCL than HS.

	+/+	+/-	-/-
n	19	18	25
Cases with observed tumors	5	10	20
Mice examined by histopathology	4	8	11
Diagnoses of HS	0	2	6
Diagnoses of HAL/HS+BCL	1	5	3
Other diagnoses	0	1	1
No significant findings	3	0	1

doi:10.1371/journal.pone.0135755.t001



This phenomenon may occur in mice as well [26]; [14], although there is also evidence that murine HS cells arise from lymphocyte-independent pathways in the liver, stemming from Kupffer cells [14] or Ly-6C+ macrophages that develop during EMH of the liver [27]. While the cellular pathway of HS development is not known, the liver is a strong candidate primary site of pathogenesis, as it is the most commonly affected organ in murine HS [28]. We found that the liver was a common site for tumors, although less common than the spleen and lymph nodes of the mesentery.

Few studies have identified genes involved in HS development [16, 29–31], however a recent forward genetics approach has identified several candidate genes altered in murine HS [32]. Canine HS studies have determined several large cytogenetic changes involved, including frequent deletions at dog chromosome 22q11, the homologous location of human chromosome 13q14, suggesting that genes in this region are implicated in canine HS development [33]. Our findings support that *Chc1L* may be a 22q11 target gene in canine HS.

Since *CHC1L* deletion likely occurs as one component in an array of mutations that develop during tumorigenesis, future studies should focus on elucidating the relationship, including possible synergy, between *Chc1L* mutation and mutation of other genes involved in cancers affected by 13q14 deletion. Other investigations may focus on extending our findings to the bedside with clinical data supportive of *CHC1L*'s role in human HS, and in understanding *CHC1L*'s molecular pathway in order to provide insight into potentially novel therapeutic targets. *CHC1L* is highly homologous to *RCC1*, the regulator of *RanGTPase*. *CHC1L* possesses two BTB/POZ domains, protein-protein interaction domains found on E3 ligase substrate adaptors. *RCBTB1*, *CHC1L*'s paralogue, interacts with *CUL3* *in vitro*, a component of E3 ligase complexes, as well as with *CHC1L* itself [34]. Therefore, it is possible that *CHC1L* may have a role as an adaptor protein, dimerizing with *RCBTB1* to regulate *RanGTPase* via ubiquitin-mediated degradation. Changes in *RanGTPase* regulation may alter nuclear trafficking and chromosome condensation, resulting in abnormal proliferation and chromosomal instability [35].

In summary, this mouse model sheds light on the function of an uncharacterized gene, providing the first direct evidence for its role as a tumor suppressor gene. Further investigation will focus confirming *CHC1L*'s role in human HS and determining its molecular pathway, with the aim of identifying therapeutically targetable pathways. Additionally, by generating *Chc1L*-conditional knockout lines, our novel mouse line may be used in future studies of HS pathogenesis, particularly with respect to literature demonstrating a putative B cell precursor to HS.

## Supporting Information

**S1 Fig. Age-matched wild-type H+E controls.** Panel 1) Spleen displaying normal architecture. Some extramedullary hematopoiesis is seen, a common finding in older mice (scale bars are 1 mm and 50  $\mu$ m). Panel 2) Lymph node with normal architecture, surrounded by mesentery (scale bars are 1 mm and 50  $\mu$ m). Panel 3) Liver with normal architecture. Mild inflammation is seen in the upper left quadrant, a common finding in older mice (scale bars are 1 mm and 50  $\mu$ m). Panel 4) Cross-section of ileum with normal architecture (scale bars are 1 mm and 50  $\mu$ m).  
(TIF)

**S1 File. ARRIVE Checklist.** Submitted as per PLOS ONE guidelines.  
(DOCX)

## Acknowledgments

We would like to thank Dr. Aaron Schimmer for his expert input in research planning, as well as the pathology core at the Center for Modelling Human Disease of the Toronto Center for Phenogenomics for providing histopathological analysis. We also acknowledge Dr. Pamela Plant and Christopher Spring for their technical assistance and their scientific insight in reviewing the manuscript.

## Author Contributions

Conceived and designed the experiments: DRS DYW SN AG ML XYW. Performed the experiments: DRS DYW YW CXS HRC HS. Analyzed the data: DRS DYW SN ML XYW. Contributed reagents/materials/analysis tools: SN ML XYW. Wrote the paper: DRS SN AG ML XYW.

## References

1. Dewald GW, Brockman SR, Paternoster SF, Bone ND, O'Fallon JR, Allmer C, et al. Chromosome anomalies detected by interphase fluorescence in situ hybridization: correlation with significant biological features of B-cell chronic lymphocytic leukaemia. *Br J Haematol*. 2003; 121(2):287–95. Epub 2003/04/16. 4265 [pii]. PMID: [12694251](#).
2. Fonseca R, Barlogie B, Bataille R, Bastard C, Bergsagel PL, Chesi M, et al. Genetics and cytogenetics of multiple myeloma: a workshop report. *Cancer Res*. 2004; 64(4):1546–58. Epub 2004/03/03. PMID: [14989251](#).
3. Cooney KA, Wetzel JC, Merajver SD, Macoska JA, Singleton TP, Wojno KJ. Distinct regions of allelic loss on 13q in prostate cancer. *Cancer Res*. 1996; 56(5):1142–5. Epub 1996/03/01. PMID: [8640774](#).
4. Della Porta M, Rigolin GM, Bugli AM, Bardi A, Bragotti LZ, Bigoni R, et al. Differentiation of follicular dendritic sarcoma cells into functional myeloid-dendritic cell-like elements. *Eur J Haematol*. 2003; 70(5):315–8. Epub 2003/04/16. 042 [pii]. PMID: [12694168](#).
5. Leroux D, Mugneret F, Callanan M, Radford-Weiss I, Dastugue N, Feuillard J, et al. CD4(+), CD56(+) DC2 acute leukemia is characterized by recurrent clonal chromosomal changes affecting 6 major targets: a study of 21 cases by the Groupe Francais de Cytogenetique Hematologique. *Blood*. 2002; 99(11):4154–9. Epub 2002/05/16. PMID: [12010820](#).
6. Elnenaï MO, Hamoudi RA, Swansbury J, Gruszka-Westwood AM, Brito-Babapulle V, Matutes E, et al. Delineation of the minimal region of loss at 13q14 in multiple myeloma. *Genes Chromosomes Cancer*. 2003; 36(1):99–106. Epub 2002/12/04. doi: [10.1002/gcc.10140](#) PMID: [12461754](#).
7. Ouillette P, Erba H, Kujawski L, Kaminski M, Shedden K, Malek SN. Integrated genomic profiling of chronic lymphocytic leukemia identifies subtypes of deletion 13q14. *Cancer Res*. 2008; 68(4):1012–21. Epub 2008/02/19. 68/4/1012 [pii] doi: [10.1158/0008-5472.CAN-07-3105](#) PMID: [18281475](#).
8. Latil A, Morant P, Fournier G, Mangin P, Berthon P, Cussenot O. CHC1-L, a candidate gene for prostate carcinogenesis at 13q14.2, is frequently affected by loss of heterozygosity and underexpressed in human prostate cancer. *Int J Cancer*. 2002; 99(5):689–96. Epub 2002/07/13. doi: [10.1002/ijc.10393](#) PMID: [12115502](#).
9. Legartova S, Hamicarova-Horakova A, Bartova E, Hajek R, Pour L, Kozubek S. Expression of RAN, ZHX-2, and CHC1L genes in multiple myeloma patients and in myeloma cell lines treated with HDAC and Dnmts inhibitors. *Neoplasma*. 2010; 57(5):482–7. Epub 2010/06/24. PMID: [20568903](#).
10. Wang J, Teves ME, Shen X, Nagarkatti-Gude DR, Hess RA, Henderson SC, et al. Mouse RC/BTB2, a Member of the RCC1 Superfamily, Localizes to Spermatid Acrosomal Vesicles. *PLoS One*. 2012; 7(6):e39846. Epub 2012/07/07. doi: [10.1371/journal.pone.0039846](#) PONE-D-12-09089 [pii]. PMID: [22768142](#).
11. Devilder MC, Cadoret E, Cherel M, Moreau I, Rondeau G, Bezieau S, et al. cDNA cloning, gene characterization and 13q14.3 chromosomal assignment of CHC1-L, a chromosome condensation regulator-like guanine nucleotide exchange factor. *Genomics*. 1998; 54(1):99–106. Epub 1998/11/10. S0888-7543(98)95498-2 [pii] doi: [10.1006/geno.1998.5498](#) PMID: [9806834](#).
12. Ohinata Y, Payer B, O'Carroll D, Ancelin K, Ono Y, Sano M, et al. Blimp1 is a critical determinant of the germ cell lineage in mice. *Nature*. 2005; 436(7048):207–13. Epub 2005/06/07. nature03813 [pii] doi: [10.1038/nature03813](#) PMID: [15937476](#).
13. Vincent SD, Dunn NR, Sciammas R, Shapiro-Shalef M, Davis MM, Calame K, et al. The zinc finger transcriptional repressor Blimp1/Prdm1 is dispensable for early axis formation but is required for specification of primordial germ cells in the mouse. *Development*. 2005; 132(6):1315–25. Epub 2005/03/08. 132/6/1315 [pii] doi: [10.1242/dev.01711](#) PMID: [15750184](#).



14. Hao X, Fredrickson TN, Chattopadhyay SK, Han W, Qi CF, Wang Z, et al. The histopathologic and molecular basis for the diagnosis of histiocytic sarcoma and histiocyte-associated lymphoma of mice. *Vet Pathol.* 2010; 47(3):434–45. Epub 2010/05/18. 47/3/434 [pii] doi: [10.1177/0300985810363705](https://doi.org/10.1177/0300985810363705) PMID: [20472805](https://pubmed.ncbi.nlm.nih.gov/20472805/).
15. Gertz MA, Greipp PR. Hematologic malignancies: multiple myeloma and related plasma cell disorders. Berlin; New York: Springer; 2004. x, 272 p. p.
16. Carrasco DR, Fenton T, Sukhdeo K, Protopopova M, Enos M, You MJ, et al. The PTEN and INK4A/ARF tumor suppressors maintain myelolymphoid homeostasis and cooperate to constrain histiocytic sarcoma development in humans. *Cancer Cell.* 2006; 9(5):379–90. Epub 2006/05/16. S1535-6108(06)00115-2 [pii] doi: [10.1016/j.ccr.2006.03.028](https://doi.org/10.1016/j.ccr.2006.03.028) PMID: [16697958](https://pubmed.ncbi.nlm.nih.gov/16697958/).
17. Martin-Caballero J, Flores JM, Garcia-Palencia P, Serrano M. Tumor susceptibility of p21(Waf1/Cip1)-deficient mice. *Cancer Res.* 2001; 61(16):6234–8. Epub 2001/08/17. PMID: [11507077](https://pubmed.ncbi.nlm.nih.gov/11507077/).
18. Mashima R, Honda K, Yang Y, Morita Y, Inoue A, Arimura S, et al. Mice lacking Dok-1, Dok-2, and Dok-3 succumb to aggressive histiocytic sarcoma. *Lab Invest.* 2010; 90(9):1357–64. Epub 2010/06/16. labinvest2010121 [pii] doi: [10.1038/labinvest.2010.121](https://doi.org/10.1038/labinvest.2010.121) PMID: [20548287](https://pubmed.ncbi.nlm.nih.gov/20548287/).
19. Jaffe ES HN, Stein H, Vardiman JW (eds). Pathology and Genetics of Tumours of Haematopoietic and Lymphoid Tissues. Haematopoietic PaGoTo, Lyon aLTI, editors2001. pp 273–90. p.
20. Feldman AL, Arber DA, Pittaluga S, Martinez A, Burke JS, Raffeld M, et al. Clonally related follicular lymphomas and histiocytic/dendritic cell sarcomas: evidence for transdifferentiation of the follicular lymphoma clone. *Blood.* 2008; 111(12):5433–9. Epub 2008/02/15. blood-2007-11-124792 [pii] doi: [10.1182/blood-2007-11-124792](https://doi.org/10.1182/blood-2007-11-124792) PMID: [18272816](https://pubmed.ncbi.nlm.nih.gov/18272816/).
21. Wang E, Papalas J, Hutchinson CB, Kulbacki E, Huang Q, Sebastian S, et al. Sequential development of histiocytic sarcoma and diffuse large b-cell lymphoma in a patient with a remote history of follicular lymphoma with genotypic evidence of a clonal relationship: a divergent (bilineal) neoplastic transformation of an indolent B-cell lymphoma in a single individual. *Am J Surg Pathol.* 2011; 35(3):457–63. Epub 2011/02/15. 00000478-201103000-00018 [pii]. PMID: [21317718](https://pubmed.ncbi.nlm.nih.gov/21317718/).
22. Zeng W, Meck J, Cheson BD, Ozdemirli M. Histiocytic sarcoma transdifferentiated from follicular lymphoma presenting as a cutaneous tumor. *J Cutan Pathol.* 2011; 38(12):999–1003. Epub 2011/09/03. doi: [10.1111/j.1600-0560.2011.01769.x](https://doi.org/10.1111/j.1600-0560.2011.01769.x) PMID: [21883369](https://pubmed.ncbi.nlm.nih.gov/21883369/).
23. Zhang D, McGuirk J, Ganguly S, Persons DL. Histiocytic/dendritic cell sarcoma arising from follicular lymphoma involving the bone: a case report and review of literature. *Int J Hematol.* 2009; 89(4):529–32. Epub 2009/04/04. doi: [10.1007/s12185-009-0300-y](https://doi.org/10.1007/s12185-009-0300-y) PMID: [19343479](https://pubmed.ncbi.nlm.nih.gov/19343479/).
24. Wang E, Hutchinson CB, Huang Q, Sebastian S, Rehder C, Kanaly A, et al. Histiocytic sarcoma arising in indolent small B-cell lymphoma: report of two cases with molecular/genetic evidence suggestive of a 'transdifferentiation' during the clonal evolution. *Leuk Lymphoma.* 2010; 51(5):802–12. Epub 2010/03/25. doi: [10.3109/10428191003699845](https://doi.org/10.3109/10428191003699845) PMID: [20331331](https://pubmed.ncbi.nlm.nih.gov/20331331/).
25. Chen W, Lau SK, Fong D, Wang J, Wang E, Arber DA, et al. High frequency of clonal immunoglobulin receptor gene rearrangements in sporadic histiocytic/dendritic cell sarcomas. *Am J Surg Pathol.* 2009; 33(6):863–73. Epub 2009/01/16. PMID: [19145200](https://pubmed.ncbi.nlm.nih.gov/19145200/).
26. Bauer SR, Holmes KL, Morse HC 3rd, Potter M. Clonal relationship of the lymphoblastic cell line P388 to the macrophage cell line P388D1 as evidenced by immunoglobulin gene rearrangements and expression of cell surface antigens. *Journal of immunology.* 1986; 136(12):4695–9. PMID: [3086440](https://pubmed.ncbi.nlm.nih.gov/3086440/).
27. Ohnishi K, Tanaka S, Oghiso Y, Takeya M. Immunohistochemical detection of possible cellular origin of hepatic histiocytic sarcoma in mice. *Journal of clinical and experimental hematopathology: JCEH.* 2012; 52(3):171–7. PMID: [23269076](https://pubmed.ncbi.nlm.nih.gov/23269076/).
28. Lacroix-Triki M, Lacoste-Collin L, Jozan S, Charlet JP, Caratero C, Courtade M. Histiocytic sarcoma in C57BL/6J female mice is associated with liver hematopoiesis: review of 41 cases. *Toxicologic pathology.* 2003; 31(3):304–9. PMID: [12746118](https://pubmed.ncbi.nlm.nih.gov/12746118/).
29. Li Z, Kustikova OS, Kamino K, Neumann T, Rhein M, Grassman E, et al. Insertional mutagenesis by replication-deficient retroviral vectors encoding the large T oncogene. *Ann N Y Acad Sci.* 2007; 1106:95–113. Epub 2007/03/31. annals.1392.003 [pii] doi: [10.1196/annals.1392.003](https://doi.org/10.1196/annals.1392.003) PMID: [17395733](https://pubmed.ncbi.nlm.nih.gov/17395733/).
30. Lund AH, Turner G, Trubetskoy A, Verhoeven E, Wientjens E, Hulsman D, et al. Genome-wide retroviral insertional tagging of genes involved in cancer in Cdkn2a-deficient mice. *Nat Genet.* 2002; 32(1):160–5. Epub 2002/08/20. [pii]. PMID: [12185367](https://pubmed.ncbi.nlm.nih.gov/12185367/).
31. Mashima R, Hishida Y, Tezuka T, Yamanashi Y. The roles of Dok family adapters in immunoreceptor signaling. *Immunol Rev.* 2009; 232(1):273–85. Epub 2009/11/17. IMR844 [pii] doi: [10.1111/j.1600-065X.2009.00844.x](https://doi.org/10.1111/j.1600-065X.2009.00844.x) PMID: [19909370](https://pubmed.ncbi.nlm.nih.gov/19909370/).
32. Been RA, Linden MA, Hager CJ, DeCoursin KJ, Abrahante JE, Landman SR, et al. Genetic signature of histiocytic sarcoma revealed by a sleeping beauty transposon genetic screen in mice. *PLoS One.*

2014; 9(5):e97280. doi: [10.1371/journal.pone.0097280](https://doi.org/10.1371/journal.pone.0097280) PMID: [24827933](https://pubmed.ncbi.nlm.nih.gov/24827933/); PubMed Central PMCID: PMC4020815.

33. Hedan B, Thomas R, Motsinger-Reif A, Abadie J, Andre C, Cullen J, et al. Molecular cytogenetic characterization of canine histiocytic sarcoma: A spontaneous model for human histiocytic cancer identifies deletion of tumor suppressor genes and highlights influence of genetic background on tumor behavior. *BMC Cancer*. 2011; 11:201. Epub 2011/05/28. 1471-2407-11-201 [pii] doi: [10.1186/1471-2407-11-201](https://doi.org/10.1186/1471-2407-11-201) PMID: [21615919](https://pubmed.ncbi.nlm.nih.gov/21615919/).
34. Plafker KS, Singer JD, Plafker SM. The ubiquitin conjugating enzyme, UbcM2, engages in novel interactions with components of cullin-3 based E3 ligases. *Biochemistry*. 2009; 48(15):3527–37. Epub 2009/03/05. doi: [10.1021/bi801971m](https://doi.org/10.1021/bi801971m) PMID: [19256485](https://pubmed.ncbi.nlm.nih.gov/19256485/).
35. Clarke PR, Zhang C. Spatial and temporal coordination of mitosis by Ran GTPase. *Nat Rev Mol Cell Biol*. 2008; 9(6):464–77. Epub 2008/05/15. nrm2410 [pii] doi: [10.1038/nrm2410](https://doi.org/10.1038/nrm2410) PMID: [18478030](https://pubmed.ncbi.nlm.nih.gov/18478030/).